ITER Divertor Performance in the Low Activation Phase

A.S. Kukushkin[1], H.D. Pacher[2], V. Kotov[3], G.W. Pacher[4], R.A. Pitts[1], D. Reiter[3]

[1]ITER Organization, Cadarache, France; [2]INRS-EMT, Varennes, Québec, Canada;
[3]FZ Jülich, Jülich, Germany; [4]Hydro-Québec, Varennes, Québec, Canada

E-mail contact of the first author: Andre.Kukushkin@iter.org

Abstract. The paper presents results of SOLPS modelling of the edge plasma performance during the low activation phase of ITER operation. The calculations show that the peak power loading of the divertor targets can reach the reactor-relevant level of 3 to 5 MW/m^2, even without the fusion reactions, rendering commissioning of the high heat flux components possible in this phase. Parameterization of the output of the SOLPS runs for the predominantly helium plasma concerned by the studies reported here is performed, thus providing the boundary conditions for modelling of the core and allowing efficient integration of the core and edge models. This approach, using the ASTRA code for core simulations, is applied to the analysis of hydrogen accumulation in helium plasmas due to H pellet injection. The latter is the only available option for early testing of ELM pace-making as an ELM control tool assuming H-mode in hydrogen will not be possible. Critical dilution with H down to 70% He in the core plasma can be reached in only 0.5 to 1 s or even shorter, depending on the assumptions made.

1. Introduction

The low activation phase of ITER operation is an important part of the ITER research plan. Only H and He are permitted as working gases during this phase so that human access to the machine is still possible, facilitating commissioning and testing of the ITER sub-systems − in particular, ELM mitigation techniques, additional heating systems and in-vessel components. Techniques to mitigate large ELMs can naturally only be tested in good H-mode plasmas with type I ELMs, requiring the heating power to be well in excess of the threshold power for the L-H transition, P_{LH}. In the absence of fusion power, this threshold must be as low as possible, especially since not all heating systems are likely to be at full capacity in the early phases of operation. Even if the full heating power is routinely achieved, the expected high P_{LH} in H and He compared with D or DT fuel means it is unlikely that H-modes can be attained at the nominal ITER plasma current (15 MA) [1].

Current experimental evidence that P_{LH} in He plasmas can be significantly lower than in H, suggests that He plasmas at half nominal current (and therefore half toroidal field, 2.65 T, which lowers P_{LH} further still) will be a prime candidate for early phase operation with well developed type I ELMs. However, He fuelling can be accomplished only by gas injection which can be rather inefficient for core fuelling in ITER [2] and He pellets are not available. To test ELM pace-making by pellet injection in He plasmas (one of the two main candidate schemes that are under consideration for ITER [3]), H pellets will therefore have to be used, implying a significant concentration of H in the “He” plasmas since core fuelling with H pellets is more efficient than that possible using He gas puffing at the edge. Furthermore, it is known that the performance of majority He edge and divertor plasmas differs from that of majority hydrogenic plasmas [4]. This is particularly true in the presence of carbon (which will be used as target material in the non-active phase), since chemical erosion does not occur for He fuel.

Initial divertor plasma modelling runs aimed at exploration of the conditions of divertor operation with predominantly He + H plasmas were reported in [2]. In the present paper, we apply the SOLPS4.3 code suite to study in a systematic (though time-averaged, i.e. no resolution of ELMs) way the operational space of the ITER divertor working with He and H

plasmas, with C and Be as the intrinsic impurities. Helium fuelling is provided in the simulations by means of gas puffing, and H can be introduced via gas puffing and/or H pellet fuelling (modelled in the SOL as an ion outflow from the core). The current reference ITER geometry ("F57" in [5]) is used in the calculations. The methodology is the same as that applied in the extensive similar work we have already undertaken to assess divertor performance and core-edge integration for the Baseline burning plasma [6, 7, 8, 9]: groups of simulations have been performed in which, for any given group, only the particle content outside the separatrix is allowed to vary ("density scans") inside the group, with all other key control parameters fixed. The other control parameters are systematically varied from group to group.

Two different strategies are used in performing the density scans for the current study. In the first (A), the only source of hydrogen is the ion flux from the core which is kept constant whereas the He puffing rate varies. This corresponds to core fuelling with hydrogenic pellets (high field side injection) at a constant rate. The second strategy, (B), prescribes − in addition to a constant H flux from the core − a simultaneous variation of the H and He gas puffing rates to keep the ratio of H to He in the total edge particle content constant. This approach has no direct projection to a realistic discharge control scheme, but it allows clearer comparison for understanding of the plasma composition effects. In both strategies, the He ion outflow from the core is adjusted to balance the He neutral influx to the core.

2. Divertor performance in helium compared to deuterium

For this analysis we compare several density scans with different H outflow from the core in majority He plasma, obtained using strategy A, with one of our standard density scans for D (representing both D and T) plasma [9] at the same power input to the SOL, P_{SOL}= 60 MW and the same constant radial diffusivities. A principal difference between He and D plasmas is a much lower level of C source from divertor target erosion since chemical erosion is absent in He. Parallel transport in He plasma is slower than in D for the same temperature because of the higher charge and mass of the He ions, and the neutral penetration in the divertor is somewhat better due to the higher ionization potential of the He atoms compared with hydrogenic species. In these He runs we consider also Be transport since its source from the first wall erosion can be comparable with the C divertor source.

The results show indeed that in He plasma, most of the edge/divertor radiation originates from He, with the C radiation contributing some 30% (except for the lowest densities where the radiation from He and C can become closely comparable, see the next section) and that from Be being negligible in the power balance. The He plasma temperature at the separatrix is higher compared with D, which can be explained by a reduction of the parallel heat conductivity and ion-electron energy exchange rate when D is replaced by He. The maximum plasma temperature at the targets, which is attained well outside the separatrix strike point position in the partially detached plasma, is higher for He + H plasmas for the same neutral pressure in the divertor p_n. The latter is measured in the private flux region (PFR) under the divertor dome, so that the higher plasma temperature at the outer part of the SOL in the divertor can be attributed to the longer mean-free path of the He atoms, which reduces the local recycling and enhances the neutral penetration to the PFR, thus increasing p_n.

Selecting p_n as the measure of the edge plasma density, we find that there is no big difference, Fig. 1a, in the maximum peak power loading of the targets q_{pk} in the He and D plasmas at the same P_{SOL} (60 MW; the standard D 100 MW case is shown for comparison) − except for the lower pressure range where the He curve is somewhat steeper. Note, however, that this

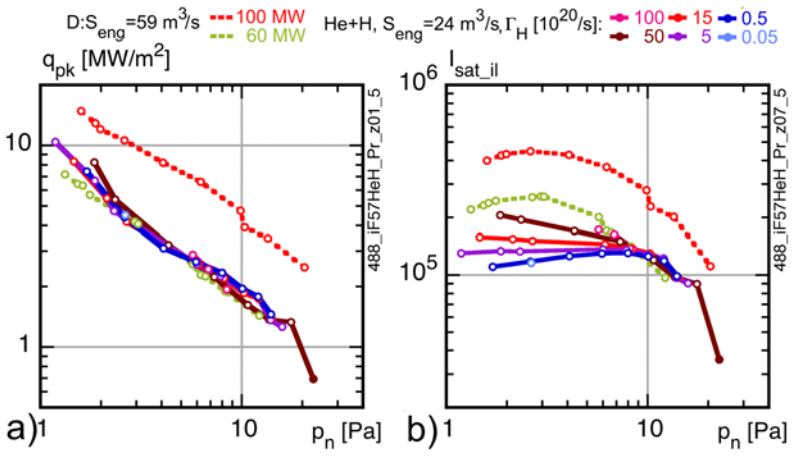

Fig. 1. Peak power loading of the targets (a) and total ion saturation current on the inner target [a.u.](b) vs. neutral pressure in PFR for D (dashed lines: red 100 MW, green 60 MW) and He with various H throughput levels (60 MW, solid lines). The lowest H flux (blue) curve corresponds to practically pure He (H contributes less than 4% to the total particle content). The I_{sat} roll-over for higher H throughput seems to occur at p_n below the considered range

maximum is located on the outer target for the low p_n values and switches to the inner when p_n increases. The difference in the q_{pk} behaviour is therefore due to the inner divertor and, because the contribution of radiation is more important at higher p_n, can be attributed to a difference in the radiation pattern between the He and D plasmas. It is worth noting that according to the simulation values of q_{pk} in the range of 3 to 5 MW/m^2 can be achieved even with rather low (60 MW) heating power in ITER, thus allowing steady state DT-phase divertor power handling to be assessed very early on. (Although Fig. 1a shows q_{pk} up to 10 MW/m^2, this corresponds to low p_n which is not compatible with the core density of 3 10^{19}m^{-3} required to avoid the neutral beam shine-through in He plasma [1]).

A roll-over of the ion saturation current (or ion flux) on the targets as density increases (as an indication of partial detachment) is not apparent at first glance (Fig. 1b). At the highest H throughput, it occurs at lower neutral pressure than in D and shifts to higher pressure for almost pure He. The reason for such a behaviour can be understood from a more systematic study of the effect of the hydrogen admixture in the He plasma.

3. H effect in the divertor plasma

Whilst the H content in the He plasma does not strongly affect the target loading, Fig. 1a, it can have other consequences. In order to separate the hydrogen and helium effects, several density scans have been run using the strategy B, namely keeping the He to H ratio in the total particle content constant. In these runs the Be component was neglected, both for simplicity and to ensure a more realistic description of C for predominantly H plasmas. Indeed, as shown in [10], the assumption of a carbon first wall leads to results close to those obtained with a more complex model taking into account carbon re-erosion from a Be wall. (A model with C sticking at a Be wall has been found in [10] to strongly underestimate the SOL carbon level.)

In these simulations the trend in the I_{sat} roll-over shown in Section 2 becomes understandable. In almost pure H it behaves similarly to that in D, Fig. 2. The values of I_{sat} for the same p_n become lower, which is consistent with better neutral penetration to the PFR in the case of H plasma. When the He percentage increases, the roll-over position shifts to progressively higher p_n (volumetric recombination is weaker in He than in H) and the I_{sat} decreases, reflecting better He atom penetration to the PFR. The H percentage in the density scans performed according to Strategy A (Section 2) is not constant: it strongly increases towards

the low pressure, low density end of the curves. Therefore an increase of p_n in Fig. 1b can be translated in terms of Fig. 2 as an increase of p_n accompanied by a transition to a curve corresponding to a lower H concentration. This reduces the target ion flux resulting in the low density roll-over seen in Fig. 1b for the high H throughput.

Another interesting effect of H in the plasma is the renewed significance of molecularly activated recombination (MAR) − a chain of reactions beginning with charge exchange between a hydrogen molecule and a hydrogen ion [11]. If the resulting molecular ion decays into two atoms, then this chain effectively transforms ions into neutrals and can be considered an effective recombination. It was shown in [12, 13] that if the excitation of the atoms resulting from decomposition of the molecular ions is taken into account, then in the temperature range over which the required charge exchange is significant, the dominant molecular ion decay channel is decomposition into an ion plus an atom and therefore the MAR effect becomes weaker than usual 3-body recombination. However, the consideration [13] was valid for the D isotope. In the case of an H^+ ion, the charge exchange rate shifts to lower temperatures because of the lower mass, and a temperature window appears in which MAR can be significant. (In practice this does not affect the results shown in Fig. 2, but makes it impossible to simulate higher densities since, in the presence of this effect, the convergence of the code requires too small time steps to balance the increase of recombination and the corresponding reduction of the ion density.)

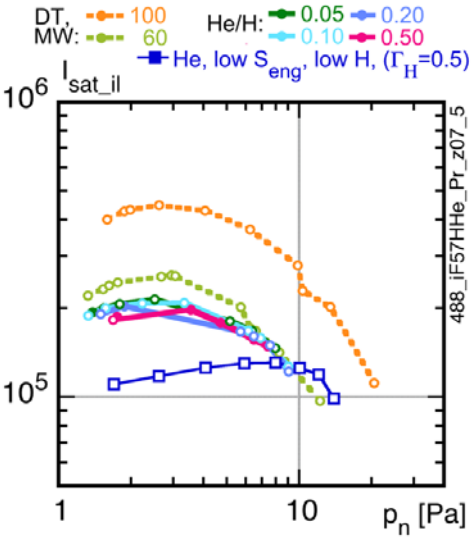

Fig. 2. Ion saturation current on the inner target vs. p_n for D (dashed lines) and H-He plasma with fixed percentage of He in the total particle content (solid lines). The highest (turquoise and green) solid curve corresponds to practically pure H, and the lowest one (blue, light line, but calculated at lower pumping speed, same as blue curve of Fig. 1b) to practically pure He. All the He+H runs are done with P_{SOL}= 60 MW.

4. Edge data scalings for predominantly helium plasmas

In order to perform computationally efficient integrated modelling describing the core, pedestal and SOL and divertor in a consistent way [8], the results of SOLPS modelling need to be expressed in terms of output parameters as functions (parameterised scalings) of the input parameters for the SOL model. This is the method previously developed for the integrated modelling of the baseline Q_{DT} = 10 inductive scenario [6−9]. These relations serve as the boundary conditions for the core model at the interface between the two regions, thus ensuring the consistency between the core and edge. This procedure effectively translates the features of the processes outside the separatrix into constraints on the core operation, screening out core solutions that would lead to unrealistic SOL conditions. The selection of which interface parameters to allocate to which parameter set (either input or output) is not unique. However, some choices are preferable for convenience in solving the equations both in the core model and in SOLPS. We follow the strategy established in [7, 9, 8] and select the energy and ion outflows across the separatrix as input and the electron and ion temperature and ion densities there, together with the neutral influxes and energies as the output parameters. In making this choice, the remaining free control parameters for the model as a whole are the extra heating and fuelling of the core, the gas puffing and the pumping speed. These are indeed amongst the principal controllable parameters in the actual experiment.

For the present scaling we use the SOLPS density scans obtained using the strategy A (Section 1) for different values of P_{SOL}, the pumping speed and the H admixture in the He plasma. We use a normalized pumping speed $S_n = S_{eng}[m^3 s^{-1}]/59$, where S_{eng} is the "engineering" pumping speed [14] in m^3/s (limited to 75 in standard ITER operation), and a normalised input power to the SOL $P_{\#} = P_{SOL}[MW]/100$ (the normalization constants correspond to the "standard" values taken for D-T plasmas [9]). Following [7] and particularly [9], the solutions are expressed in terms of μ – the neutral pressure in the divertor, normalised so that detachment corresponds to $\mu = 1$. (Detachment is in turn defined here as that pressure for which the total ion flux to either divertor drops down to 80% of its rollover value, [9]). For the He-H plasmas, this is found to be

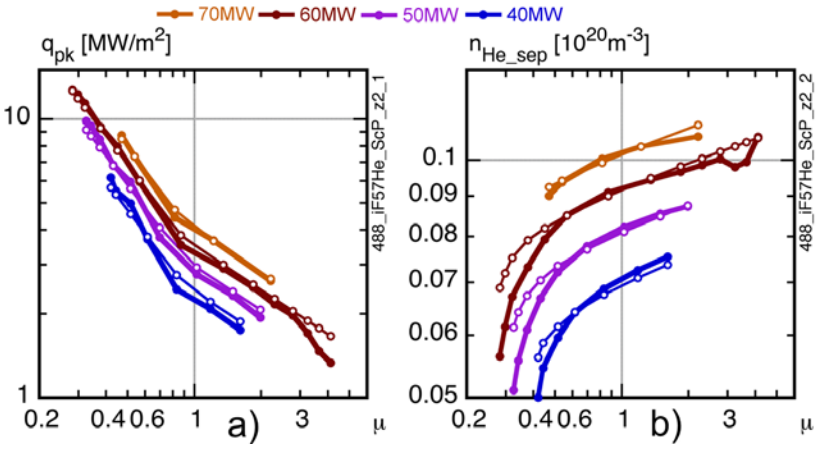

Fig. 3. Peak power load (a) and He ion density at the separatrix (b) versus normalised pressure μ for He plasmas at SOL power of 40 (lowest) to 70 (highest) MW. Simulations are the solid lines, filled symbols; fit points (the scalings) are the light lines, hollow symbols.

$$\mu = 0.075 P_{\#}^{-1.05} \left(\left(\Gamma_{He} + 0.2\Gamma_H \right) / S_n \right)^{0.62}, \tag{1}$$

quantifying the transition of the ion saturation current from dominant He to dominant H plasma discussed in Section 3.

The peak power load is found to shift from the inner divertor at low p_n to the outer as p_n rises (change of slope in Fig. 3a). This, and the power dependence, can be expressed by:

$$q_{pk} = P_{\#}^{0.93} \max\left\{ 5.3\,\mu^{-1.06}, 5.66\,\mu^{-0.53} \right\} \tag{2}$$

The average helium separatrix density varies strongly with power but weakly with the other parameters including the H fuelling, at least for the higher levels of μ (Fig. 3b).

$$n_{He\_sep} = 0.13\, P_{\#}^{0.66} \mu^{0.1} S_n^{0.025} \left(1 + 0.03 \left(\Gamma_H / \Gamma_{He} \right) \right)^{-1} \tag{3}$$

The separatrix densities of the other species are found to be fitted by:

$$n_{H\_sep} = 0.0034 \left(\Gamma_H / \left(S_n \mu \right) \right)^{0.86}, \qquad n_{Be\_sep} = 1.1 \cdot 10^{-4} P_{\#}^{0.66} \mu^{0.65} S_n^{0.33} \tag{4}$$

$$n_{C\_sep} = 8.5 \cdot 10^{-5} \left(\Gamma_{He} / \left(24 S_n \right) \right) \mu^{-3.17} + 3.8 \cdot 10^{-4} \left(\Gamma_H / \left(24 S_n \right) \right)^{1.5} \mu^{-1.56} \tag{5}$$

yielding a total ion density at the separatrix:

$$n_{i\_sep} = n_{He\_sep} + n_{H\_sep} + n_{Be\_sep} + n_{C\_sep} \tag{6}$$

The charge state of each impurity species at the separatrix is found to be practically constant (values as in Eq. 7), so that the fitted electron density is given by

$$n_{e\_sep} = 2 n_{He\_sep} + n_{H\_sep} + 3.9 n_{Be\_sep} + 5.5 n_{C\_sep} \tag{7}$$

It is found that in the simulations $n_{i\_sep} T_{i\_sep}$ and $n_{e\_sep} T_{e\_sep}^{5/2}$ depend only on the power, so that the separatrix ion and electron temperatures are given by:

$$T_{i\_sep} = 78\, P_{\#}^{1.0} n_{i\_sep}^{-1}, \qquad T_{e\_sep} = 124 P_{\#}^{0.56} n_{e\_sep}^{-0.4} \tag{8}$$

and the influx and effective temperatures of the neutrals crossing the separatrix are

$$\Gamma_{H\_sep} = 0.007\ P_{\#}^{-2.1}\mu^{-1.13}\left(\Gamma_H / S_n\right), \qquad \Gamma_{He\_sep} = 7.0\mu^{0.8}\left(1+0.22\left(\Gamma_H/\Gamma_{He}\right)\right)^{-1} \tag{9}$$

$$\Gamma_{Be\_sep} = 0.008, \quad \Gamma_{C\_sep} = 0, \qquad T_{H\_sep} = 0.5T_{i\_sep}, \qquad T_{He\_sep} = 30$$

All the densities in these equations are in 10^{20}m^{-3}, the particle fluxes in Pa-m^3/s, the temperatures in eV and the $q_{\rm pk}$ in MW/m^2. Γ_H and Γ_{He} in Eqs. (1−9) are the total pumping throughput of H and He particles. The quality of the scalings is illustrated in Fig. 3.

5. H accumulation in the core

One of the principal questions to be answered by this type of modelling is the strength of core fuelling necessary to obtain the desired density control in the discharge. Moreover, as pointed out in Section 1, pellet fuelling in ITER He plasmas will only be possible with H pellets, resulting in dilution of the He plasma. This in turn will deteriorate the H-mode conditions [15] required to produce the very ELMs that are mandatory to perform tests of the pellet ELM-pacing scheme which is one of the goals of the ITER non-active phase experiments. Studies on ASDEX Upgrade indicate that an H admixture does not affect the L-H threshold until $\zeta_{\rm He} = n_{\rm He}/(n_{\rm He}+ n_{\rm H})$ drops below 70% but then there is a deterioration of the H-mode quality [16]. Estimating the H accumulation in the core is thus very important for the evaluation of the potential of He plasmas for H-mode testing in the non-active phase.

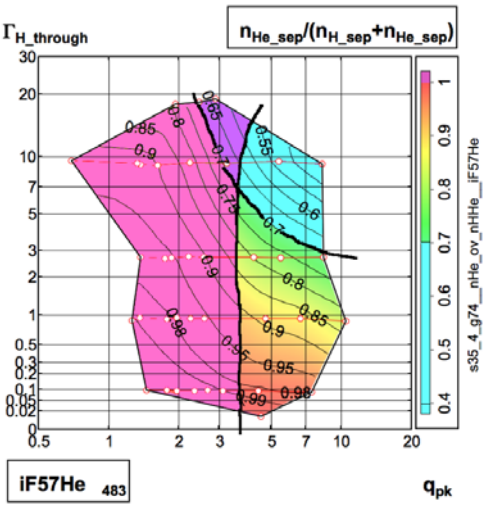

Fig. 4. Steady state separatrix He fraction as a function of H throughput and peak power load for engineering pumping speed 24 m^3/s. Shaded areas indicate $\mu > 1$ (pink), He fraction < 0.7 (turquoise), or both simultaneously (purple)

An initial indication based only on the SOL scaling may be found in Fig. 4. For an engineering pumping speed of 24 m^3/s and plasmas which are not detached, the steady state H throughput cannot exceed 7 Pa-m^3/s at 3.5 MW/m^2 (or 3 Pa-m^3/s at 10 MW/m^2) if $\zeta_{\rm He}$ at the separatrix is not to fall below 0.7. Since a larger value of H throughput is desirable for commissioning the pace-making system, and because direct core fuelling is only possible with H so that the core $\zeta_{\rm He}$ will be even lower ($\zeta_{\rm He}$= 0.48 for the former case above in steady state and with moderate pinch, c=0.5, see next paragraph), H throughput is optimised for the following core transport simulations by increasing the pumping speed to 75 Pa-m^3/s.

Since the H accumulation in the core also depends on the core transport, the modelling work necessarily involves development and application of a consistent core-edge model for the low-activation phase plasmas. Here we follow the philosophy of [8] using the parameterized results of the SOLPS modelling (Section 4) as the boundary conditions for a time-dependent, 1D core-and-pedestal model. The latter includes the core transport of energy (MMM model) and particles ($D_\perp = 0.1(\chi_{\perp e}+ \chi_{\perp i})$ throughout the core), with the pedestal formed by reduction of the transport coefficients in the edge (at locations where a criterion for suppression of the plasma instabilities is satisfied), and the pressure gradient limited to the ballooning limit (see Ref. [8] for the details). The particle sources are the neutral fluxes of He and H across the separatrix as obtained from the SOLPS results with an addition due to the H pellet fuelling. They are represented simply by an H particle source with fall-off length of 0.4 m from the

separatrix inward, set at 1 Pa·m^3/s initially and sharply increased to 10 Pa·m^3/s after reaching steady state to mimic the ELM pace-making. Since current experiments indicate that an anomalous inward pinch may exist, but no reasonable model for this pinch is available, we consider three different cases for which an extra pinch velocity, $v_p = c(2r/a^2)D_\perp$ is applied to all species, with c taking the values 0, 0.5 and 1. In the course of this evolution, the helium puffing rate is adjusted to maintain either q_{pk} = 5 MW/m^2 or μ = 1, the highest pressure before full detachment. The plots below show the second, less demanding, option, for which q_{pk} ~ 3.5 MW/m^2.

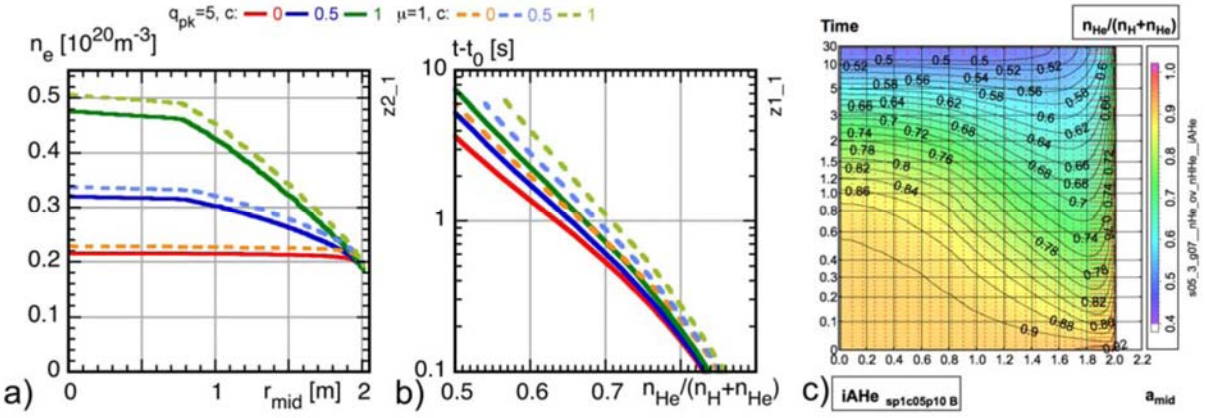

Fig. 5. (a) Radial profile of stationary electron density for either q_{pk} = 5 or μ = 1 (see text), for pinch factors c=0,0.5,1; (b) time to reach a given value of ζ_{He} anywhere in the profile; (c) evolution of the He concentration profile in time for c = 0.5, μ = 1. Zero time corresponds to the start of enhanced fuelling.

In the absence of an anomalous pinch the density profiles in the core are flat and some (hydrogen) pellet fuelling is required to sustain the minimum $n_e = 3\cdot10^{19}$m^{-3} necessary to avoid beam shine-through [1]. However, with a moderate pinch (c = 0.5) the steady-state density profile in He just exceeds this value without H pellet fuelling, Fig. 5a. As the H pellet fuelling increases, the core electron density increases but the helium fraction ζ_{He} decreases, Fig. 5c. It is not clear where the critical He fraction ζ_{He}=0.7 should be taken; according to [16] it should be at the edge rather than deep in the core (top of the pedestal?). Taking, conservatively, the minimum value across the core, one can see from Fig. 5c that ζ_{He} = 0.7 can be reached in 0.9 s if c = 0.5 for the case shown there. Fig. 5b shows the time at which a given minimum He concentration is reached for the different pinch coefficients and control parameters. With the μ = 1 condition and a stronger pinch (c = 1), this time to reach ζ_{He} = 0.7 can be as high as 1 s, whereas without the pinch (c = 0) it drops to about 0.7 s and further still to 0.5 s if the higher q_{pk} condition, q_{pk} = 5 MW/m^2, needs to be sustained for commissioning. If the critical He fraction to maintain H mode were lower than the ζ_{He} = 0.7 indicated by ASDEX Upgrade, the times would be longer (Fig. 5b).

Although durations in the range 0.5 – 1.0 s would be sufficient to test the ELM pellet pacing technique to some degree (given the paced ELM frequencies that the ITER system must deliver of several tens of Hz), it is clearly insufficient for larger scale testing, in which the entire system (injector, plasma, plasma-surface interaction) would come into equilibrium. Note that these estimates are done for the H fuelling rate corresponding to the lower range of the throughput required for the pace-making. The upper estimate for this required throughput is a factor 3 higher [17]; for that throughput the time to reach ζ_{He} = 0.7 is evaluated to be much shorter, of the order of 0.1 seconds depending on the case.

6. Conclusions

An extensive modelling study of He majority plasma in ITER has shown differences in divertor operation with He-H compared to D-T plasma, most of which are qualitatively understood. An important message from this study is that the power loading on the targets can reach levels relevant to those expected during burning plasma operation, even in He plasma and with the relatively low heating power that is expected to be available during the non-active phase of ITER operation. It will therefore be possible to perform a reasonable degree of high heat flux component testing, even in this phase.

The results of divertor modelling are parameterized to produce a set of effective boundary conditions that can be used to constrain a core transport model. Applying this integrated model of the whole plasma in ITER to the problem of core hydrogen accumulation by pellet injection into a majority He plasma shows that for an H throughput of 10 $Pa \cdot m^3/s$ at 75 m^3/s pumping speed, the dilution by H can reach significant levels in times of only 0.5 – 1 s or even shorter, depending on the assumptions made. This is probably marginally sufficient for basic commissioning of the Type I ELM pellet pace-making technique in helium H-mode plasma.

Therefore, while it is unlikely that the He plasma can provide conditions permitting full-scale testing of ELM pace-making during the non-active phase, these simulations show that commissioning of this system can still be possible.

The views and opinions expressed herein do not necessarily reflect those of the ITER Organization

[1] A. Polevoi, D. Campbell, V.A. Chuyanov, et al., Proc. 22nd Fusion Energy Conference, Geneva, 2008, paper IAEA-CN-165/IT/P6-11

[2] A.S. Kukushkin, H.D. Pacher, V. Kotov, et al., Proceedings of the 36th EPS Conference on Controlled Fusion and Plasma Physics, Sofia, 2009, paper P-4.167.

[3] A. Loarte, D. Campbell, Y. Gribov, et al., paper ITR/1-4 at this conference

[4] R. A. Pitts, P. Andrew, Y. Andrew, et al., *J. Nucl. Mater*. **313-316** (2003) 777

[5] A.S. Kukushkin, H.D. Pacher, A. Loarte, et al., *Nucl. Fusion* **49** (2009) 075008

[6] A.S. Kukushkin, H.D. Pacher, G.W. Pacher, et al., *Nucl. Fusion* **43** (2003) 716

[7] H.D. Pacher, A.S. Kukushkin, G.W. Pacher, et al., *J. Nucl. Mater.*, **390−391** (2009) 259

[8] G.W. Pacher, H.D. Pacher, G. Janeschitz, A.S. Kukushkin, *Nucl. Fusion* **48** (2008) 105003

[9] H.D. Pacher, A.S. Kukushkin, G.W. Pacher, et al., Proc. 19th PSI Conference, San Diego, 2010 (to appear in *J. Nucl. Mater*.)

[10] A.S. Kukushkin, H.D. Pacher, D.P. Coster, et al., *J. Nucl. Mater*. **337–339** (2005) 50

[11] S.I. Krasheninnikov, A.Yu. Pigarov and D.J. Sigmar, *Phys. Lett. A* **214** (1996) 285

[12] D. Reiter, Chr. May, M. Baelmans, P. Börner, *J. Nucl. Mater*. , **241-243** (1997) 342

[13] A.S. Kukushkin, H.D. Pacher, V. Kotov, et al., *Nucl. Fusion* **45** (2005) 608

[14] A.S. Kukushkin, H.D. Pacher, V. Kotov, et al., *J. Nucl. Mater*. **363-365** (2007) 308

[15] F. Ryter, T. Pütterich, M. Reich, et al, *Nucl. Fusion* **49** (2009) 062003

[16] F. Ryter, *private communication, 2010*

[17] A.S. Kukushkin, H.D. Pacher, V. Kotov, et al., Proc. 19th PSI Conference, San Diego, 2010 (to appear in *J. Nucl. Mater*.)